Phase separation and internal strains in the mixed $La_{0.5}R_{0.5}Ba_2Cu_3O_y$ compounds (R = rare-earth element)

M. Calamiotou and A. Gantis
Solid State Physics Section, Department of Physics, University of Athens, GR-157 84 Athens, Greece

D. Palles, D. Lampakis, and E. Liarokapis
Department of Physics, National Technical University, GR-157 80 Athens, Greece

A. Koufoudakis
Institute of Materials Research, NCSR ''Democritos'', GR-15310 Aghia Paraskevi, Attiki, Greece
(Received 28 January 1998)

The mixed phase $La_{0.5}R_{0.5}Ba_2Cu_3O_y$ (where R is yttrium or another rare earth) has been prepared using a variation of the solid-state reaction technique. X-ray diffraction and Raman measurements have been carried out to study the effect of the mixed rare-earth substitution at the site of the Y atom. The x-ray-diffraction measurements show characteristic changes in the interatomic distances, which are indicative of strains in the unit cell. A strain-relaxation mechanism is proposed, attributed to the separation of phases. In the micro-Raman spectra, an increase of the A_g mode frequency of the apex oxygen with increasing average La-R ionic radius is observed, the mode frequencies corresponding to the Ba and the Cu(2) atoms remain practically unaffected, while in some compounds a new mode appears at $\sim$126 cm^{-1}. The in-phase vibrations of the plane oxygen atoms show a shift to a lower frequency compared with the $RBa_2Cu_3O_y$ samples, similar to the one observed in the overdoped $YBa_2Cu_3O_y$ ($y \geq 6.92$) system. Besides, the width of this phonon is considerably larger than in the $YBa_2Cu_3O_y$ compounds, attributable to the existence of phases with underdoped, optimally doped, and overdoped oxygen concentration. As concerns the changes induced in the B_{1g} Raman active mode of the out-of-phase vibrations of the plane oxygen atoms, they are indicative of phases rich in either La, R, or an intermediate phase. Differences observed from the $Pr_{1-x}R_xBa_2Cu_3O_y$ compounds prove that the phase formation mechanism is not a pure ion-size effect. [S0163-1829(98)03645-5]

I. INTRODUCTION

The replacement of Y by a rare-earth element in the superconductor $YBa_2Cu_3O_y$ has been studied extensively in connection with the internal chemical pressure induced by the rare-earth element and the discovery that Pr affects appreciably the transition temperature T_c destroying superconductivity when added in considerable amounts.[1] The actual role of Pr in the $PrBa_2Cu_3O_y$ system is still unclear and some measurements even questioned this ability of Pr to destroy the superconductivity if it is substituted only for Y,[2] though other measurements show that when Pr is substituted for Ba it behaves in a manner similar to any other rare earth.[3] In the mixed compounds $Pr_{1-x}R_xBa_2Cu_3O_y$ the T_c was found to decrease with increasing amount of Pr, while the maximum value of x for the disappearance of superconductivity depends on the difference in the ionic radii of Pr and the other rare earth R.[1] In the Raman study of the $Pr_{0.5}R_{0.5}Ba_2Cu_3O_y$ (Pr-R123) series,[4] the phonon of B_{1g} symmetry due to the out-of-phase vibrations along the c axis of the oxygen planes was strongly influenced by the substitution. The changes in the phonon width have been attributed to the existence of phases that are rich in the two rare-earth atoms (Pr and R) and are produced when the difference of the ionic radii exceeds a value that corresponds to the reappearance of superconductivity in the compounds.[4]

In this work we study a similar series of mixed rare-earth samples where Pr has been substituted by La (known not to affect the superconductivity property and being of a size slightly larger than Pr) in order to examine the relation between phase separation, superconductivity, and size of the ion. Characteristic changes are detected in some of the Raman-active phonons in the La-R123 compounds that are similar to the ones in Pr-R123, but the appearance of phases in this type of materials seems to be more involved than originally thought.[4,5] The x-ray-diffraction (XRD) data also reveal a different behavior for the dependence of the interatomic distances on the average ionic radius of the La-R123 system, as compared with the Pr-R123 compound.[5]

II. EXPERIMENT

Polycrystalline ceramic $La_{0.5}R_{0.5}Ba_2Cu_3O_y$ (R = Lu, Yb, Tm, Er, Ho, Y, Dy, Gd, Eu, Sm, Nd, Pr) samples have been prepared by the solid-state reaction technique using stoichiometric high-purity oxide and carbonate starting materials. It is known that the chemistry of the La-Ba-Cu-O system is different from that of yttrium and most other lanthanide elements having a large number of ternary compound and solid solution series.[6,7] Sintering in inert atmosphere is necessary for the synthesis of good quality $LaBa_2Cu_3O_y$.[8–10] Therefore, sintering of the mixed $La_{0.5}R_{0.5}Ba_2Cu_3O_y$ (La-R123) series has been performed in both inert helium and oxygen atmosphere. After heating the initial La_2O_3 powder, all starting materials have been mixed, ground, pressed into pellets,

and calcinated at 920 °C. The pellets have been reground, repressed, and further thermally treated (four times) at temperatures of 940, 960, 980, and 990 °C in an oxygen atmosphere. XRD examination has shown that the pellets consisted of a single crystalline phase and the commonly found $BaCuO_2$ intermediate phase. Sintering of the samples has been further performed in He atmosphere at 950 °C for about 44 h followed by an 18-h-long sintering in O_2 atmosphere. The samples have been then furnace cooled to 500 °C and annealed at 500 °C for 24 h. The process (sintering and annealing) has been repeated until the amount of $BaCuO_2$ was asymptotically reduced to a constant value that depends on the rare-earth constituent. Although we did not perform oxygen content analysis, it is worth noticing that according to Wada *et al.*[9] for $La_{1+x}Ba_{2-x}Cu_3O_y$, the oxygen content depends on the sintering temperature: for samples sintered at 970–980 °C it is about 6.95 and for samples sintered at 900 °C it is larger than 7.0, typically about 7.15. Based on this work and the sintering procedure we have followed, one can deduce that the expected oxygen concentration of our samples should be in the range of overdoping, a hypothesis that agrees with the Raman results, as explained below.

Magnetic characterization of the samples with a standard VSM magnetometer has shown that all samples, except for the $La_{0.5}Pr_{0.5}Ba_2Cu_3O_y$ compound that has not shown any sign of superconductivity down to 4 K, are superconducting with $T_{c,\mathrm{onset}}$ ranging between 86.7 K for Lu to 90.1 K for Nd (Table I). The transitions to the superconducting state are rather broad with steplike behavior and the corresponding shielding signals are weak for all samples; these facts are indicative of the coexistence of at least two phases as far as their superconductive properties are concerned.

X-ray-diffraction patterns ($2\vartheta = 20° - 70°$) have been measured on a Siemens D5000 powder diffractometer with Cu-$K\alpha$ radiation at room temperature. Rietveld analysis of the pattern has been carried out with the program RIET.[11]

The materials have been measured by micro-Raman spectroscopy, in a Jobin-Yvon T64000 triple spectrometer equipped with a liquid-nitrogen-cooled charge coupled device (CCD) and a microscope. The beam of an Ar^+ ($\lambda = 514.5$ and 488.0 nm) laser at a power of <0.2 mW was focused to a spot of diameter 1–2 μm. A polarizer and an analyzer were employed for the application of the selection rules. Typical measurement times were 3600–7200 sec. The four A_g symmetry phonons as well as the B_{1g} phonon were observed in the $y(zz)\bar{y}$ and $y(xx)\bar{y}$ polarization configurations, respectively. The direction y of the incident and scattered light was chosen in the a-b plane and the z axis was parallel to the c axis. The directions in parentheses refer to the light polarization.

III. RESULTS AND DISCUSSION

A. Crystallographic data

The XRD patterns of all samples were indexed according to the orthorhombic space group *Pmmm.* Rietveld refinement has been carried out using the starting model of Y123 (Ref. 12) and a split Pearson VII profile shape function.[13] The structure of $BaCuO_2$ was included in the refinement with the crystallographic data given in Ref. 14. The presence of $BaCuO_2$ in our samples (Table I) was an indication for a partial substitution of La and/or the other rare earth for Ba. In this case the formed $R_{1+z}Ba_{2-z}Cu_3O_y$ phase exhibits an orthorhombic to tetragonal structural phase transition at a z value between 0.1 and 0.2 for $R=$La and between 0.2 and 0.3 for $R=$Nd, Sm, Eu.[6,9] We have tried to refine our data with a tetragonal space group but this resulted in a considerable deterioration of the R_{Bragg} factor. From this we can estimate that in our samples the substitution for Ba is kept below those values.

For the compounds with $R=$Lu, Yb, Tm, Er, Ho, Y, where the difference in electrons between R and La is expected to be detectable by x rays, the occupation factors of the rare-earth site were also refined. The results showed that the mixed-phase $La_{0.5}R_{0.5}Ba_2Cu_3O_y$ expected by the preparation stoichiometry was obtained for all samples except Ho, where considerable deviations have been detected from the nominal composition (Table I).

Table I presents the structural parameters of the investigated samples as determined from the Rietveld refinement. Bond lengths have been calculated using the program DISTAN and are presented in Table II. The amount of $BaCuO_2$ obtained from the Rietveld refinement ranges between 4.9 and 12.3%. The unit-cell parameters of the mixed La-R123 (except La-Pr123) compounds satisfy the well-known condition $a<b<c/3$, contrary to the case of the Pr123 and Pr-R123 compounds.[5]

Figure 1 shows the dependence of the a, b, and c unit-cell parameters on the rare-earth ionic radius for the mixed La-R123 in comparison with the $RBa_2Cu_3O_y$ (R123) compounds.[5] Since XRD probes the average cell structure in the mixed La-R123 compounds, the average ionic radii have been used for La and R with oxidation number $+3$ and eightfold coordination.[15] The straight line is the linear fit to the R123 data, excluding the Pr123 and La123 data. The unit-cell parameters a, b, and c in general show the expected lanthanide contraction behavior, i.e., they exhibit a linear relationship when plotted versus the average ionic radii for trivalent rare-earth ions with coordination number eight. The a and b unit-cell parameters fit to the straight line for the R123 compounds. The values of the c parameter are more scattered than those of a and b but a systematic deviation towards higher values has been obtained for compounds with an approximate average ionic radius greater than 1.09 Å, which corresponds to the mixed compound La-Y123. The La-Pr123 compound is an exception having a lower c-axis value than expected, in agreement with results reported in Ref. 5. It is worth noticing that all the mixed Pr-R123 compounds have systematically lower values for the c axis compared to the pure R123 (open triangles in Fig. 1).

The orthorhombicity of all samples is rather high, ranging between 56 and 86%. The values of orthorhombicity follow the expected decrease with increasing ionic radius as with the R123 compounds.

The c-axis dilation for the isostructural R123 compounds is a result of the interatomic bond length changes, especially the expansion of the central channel of the unit cell where the rare-earth ion is situated. Moreover, the enhanced dilation of the c unit-cell parameter that we have observed for the first members of the rare-earth atoms (Pr, Nd, Sm, Eu, Gd, Dy) of the mixed La-R123 compounds should be a manifestation of additional strains that are present in the

TABLE I. Rietveld refinements of XRD data for $La_{0.5}R_{0.5}Ba_2Cu_3O_y$. The space group used is *Pmmm* with Ba($\frac{1}{2},\frac{1}{2},z$), La($\frac{1}{2},\frac{1}{2},\frac{1}{2}$), R($\frac{1}{2},\frac{1}{2},\frac{1}{2}$), Cu1(0,0,0), Cu2(0,0,$z$), O1(0,0,$z$), O2(0,$\frac{1}{2}$,$z$), O3($\frac{1}{2}$,0,$z$), and O4(0,$\frac{1}{2}$,0).

	R=Lu	Yb	Tm	Er	Ho	Y	Dy	Gd	Eu	Sm	Nd	Pr
z (Ba) (Å)	0.1804(6)	0.1814(3)	0.1824(4)	0.1819(4)	0.1814(4)	0.1815(4)	0.1804(5)	0.1811(5)	0.1811(4)	0.1812(3)	0.1794(5)	0.1777(6)
z (Cu2) (Å)	0.353(1)	0.351(1)	0.353(1)	0.353(1)	0.351(1)	0.349(1)	0.345(2)	0.349(1)	0.347(1)	0.3459(7)	0.347(2)	0.345(1)
z (O1) (Å)	0.161(4)	0.163(3)	0.159(4)	0.162(4)	0.163(4)	0.155(4)	0.163(5)	0.163(4)	0.163(4)	0.161(4)	0.163(4)	0.162(4)
z (O2) (Å)	0.361(4)	0.369(3)	0.381(3)	0.379(3)	0.364(3)	0.383(2)	0.378(3)	0.357(4)	0.355(4)	0.356(3)	0.354(4)	0.346(4)
z (O3) (Å)	0.376(3)	0.379(2)	0.378(2)	0.383(2)	0.382(2)	0.381(2)	0.389(2)	0.396(2)	0.401(2)	0.396(2)	0.399(3)	0.393(2)
a (Å)	3.8480(4)	3.8405(3)	3.8440(4)	3.8477(2)	3.8522(4)	3.8393(3)	3.8618(4)	3.8545(4)	3.8664(4)	3.8685(4)	3.8759(4)	3.8763(4)
b (Å)	3.9047(5)	3.9012(5)	3.9039(5)	3.9066(3)	3.9099(5)	3.9057(6)	3.9183(6)	3.9129(5)	3.9175(5)	3.9203(4)	3.9263(6)	3.9207(4)
c (Å)	11.729(2)	11.712(1)	11.726(2)	11.732(1)	11.746(2)	11.719(2)	11.752(2)	11.756(2)	11.779(2)	11.784(1)	11.767(2)	11.741(1)
R (%)	5.35	6.22	4.54	5.21	5.92	4.57	5.95	5.70	6.54	6.04	6.53	8.67
R_{wp} (%)	5.75	6.35	5.40	5.79	6.18	5.33	6.27	5.98	6.60	6.47	7.12	7.43
R_{exp} (%)	3.65	4.08	3.80	3.95	3.96	3.76	4.02	3.83	4.01	3.88	4.02	3.68
R_{Bragg} (%)	7.79	7.60	5.20	5.68	7.76	4.73	8.05	7.41	9.01	6.96	8.67	8.64
$BaCuO_2$ (%)	5.68	12.34	6.37	5.63	6.91	9.73	7.08	6.16	8.98	7.81	4.89	3.59
n (La) (%)	52.5	52.4	51.0	55.3	77.0	54.2						
n (Re) (%)	47.5	47.6	49.0	44.7	23.0	45.8						
$T_{c,\ onset}$ (K)	86.7	81.2	84	87	86.5	84	89.7	87.6	87.7	89.5	90.1	

TABLE II. Bond lengths and characteristic crystallographic parameters of the $La_{0.5}R_{0.5}Ba_2Cu_3O_y$ orthorhombic compounds. Distances are in Å and angles in degrees.

	R=Lu	Yb	Tm	Er	Ho	Y	Dy	Gd	Eu	Sm	Nd	Pr
R-O(2)×4	2.52(3)	2.46(2)	2.38(2)	2.39(2)	2.50(2)	2.36(1)	2.41(2)	2.56(3)	2.58(3)	2.57(2)	2.61(3)	2.31(1)
R-O(3)×4	2.44(2)	2.41(1)	2.42(1)	2.39(1)	2.40(1)	2.40(1)	2.35(1)	2.31(1)	2.28(1)	2.31(1)	2.27(2)	2.67(3)
Ba-O(1)×4	2.751(4)	2.746(3)	2.753(5)	2.752(4)	2.753(4)	2.756(5)	2.758(4)	2.755(4)	2.760(4)	2.764(4)	2.765(3)	2.766(3)
Ba-O(2)×2	2.86(4)	2.92(3)	3.02(3)	3.01(3)	2.88(3)	3.04(2)	3.02(3)	2.83(4)	2.82(3)	2.83(3)	2.84(3)	2.79(3)
Ba-O(3)×2	3.01(3)	3.03(2)	3.01(2)	3.06(2)	3.06(2)	3.05(2)	3.14(2)	3.20(2)	3.25(2)	3.20(2)	3.23(3)	3.19(3)
Ba-O(4)×2	2.860(5)	2.864(3)	2.876(4)	2.873(4)	2.872(4)	2.865(4)	2.868(4)	2.872(4)	2.879(4)	2.881(3)	2.866(4)	2.848(4)
Cu(1)-O(1)×2	1.89(5)	1.91(4)	1.86(5)	1.90(5)	1.92(5)	1.82(5)	1.92(6)	1.92(5)	1.92(5)	1.90(5)	1.92(5)	1.90(5)
Cu(1)-O(4)×2	1.952	1.951	1.952	1.953	1.955	1.953	1.959	1.957	1.959	1.960	1.963	1.965
Cu(2)-O(1)×1	2.25(5)	2.20(4)	2.28(5)	2.24(5)	2.21(5)	2.27(5)	2.14(6)	2.19(5)	2.17(5)	2.18(5)	2.17(5)	2.15(5)
Cu(2)-O(2)×2	1.955(2)	1.962(4)	1.979(6)	1.977(6)	1.961(3)	1.993(5)	1.997(8)	1.959(2)	1.961(2)	1.964(2)	1.940(2)	1.938(2)
Cu(2)-O(3)×2	1.943(5)	1.948(4)	1.944(4)	1.956(5)	1.960(5)	1.956(5)	1.999(9)	2.005(7)	2.035(8)	2.022(7)	2.06(1)	2.045(7)
Cu(1)-Cu(2)	4.14(1)	4.11(1)	4.14(1)	4.14(1)	4.12(1)	4.09(1)	4.05(1)	4.10(1)	4.09(1)	4.076(8)	4.08(2)	4.05(2)
Cu(2)-Cu(2)	3.45(2)	3.49(2)	3.45(2)	3.45(2)	3.50(2)	3.54(2)	3.64(3)	3.55(2)	3.60(2)	3.63(1)	3.60(3)	3.64(2)
Cu(2)-O(2)-Cu(2)	174.5(2)	167.7(3)	160.9(4)	162.3(4)	171.1(2)	156.9(4)	157.6(5)	174.5(2)	174.5(2)	173.1(2)	175.1(2)	179.0(2)
Cu(2)-O(3)-Cu(2)	164.0(4)	160.6(3)	162.7(3)	159.3(3)	158.6(3)	157.9(3)	150.0(5)	148.0(5)	143.6(5)	146.1(5)	145.4(8)	148.0(8)

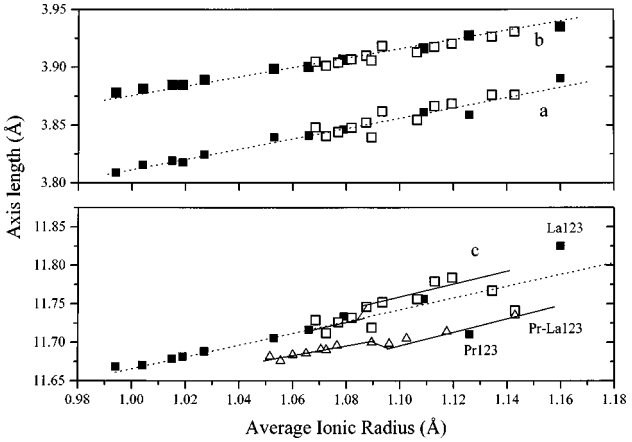

FIG. 1. Dependence of the *a*, *b*, and *c* parameters of the La-*R*123 (open squares) compounds investigated on the average ionic radius compared to the *R*123 (solid squares) and the Pr-*R*123 data (open triangles) from Ref. 5. The dotted lines are the least-squares linear fit to the *R*123 data. For the *c* axis the La123 and Pr123 data have been excluded from the linear fit.

mixed compounds. In order to have an insight in the strains of the unit cell we have calculated the different interatomic distances presented in Table II with the oxygen atoms labeled as follows: O(1) apical, O(2) plane along the *b* axis, O(3) plane along the *a* axis, and O(4) and O(5) basal plane along the *b* and *a* axis, respectively. The XRD data resulted in significant uncertainties concerning the positions of both the apical O(1) and the plane O(2,3) oxygen atoms. This may be related to the existence of more than one phases with different rare-earth and/or oxygen concentrations as was evidenced from the magnetic measurements and the Raman results that will be discussed later. Despite these uncertainties the relevant data discussed below show systematic deviations when compared with the *R*123 data.

Figure 2 shows the expansion of the central channel Cu(2)-Cu(2′) of the unit cell and the dependence of the Cu(1)-Cu(2) bond-length distance on the average ionic radius r_R. The distance Cu(2)-Cu(2′) is particularly sensitive to the lanthanide contraction, since the rare-earth ions are situated between the CuO_2 planes. It is clear from the plots of Fig. 2 that the data fit together with those of the single

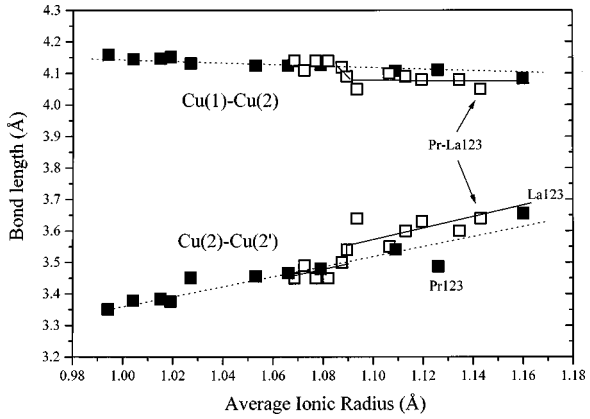

FIG. 2. Dependence of the Cu(2)-Cu(2′) and Cu(2)-Cu(1) distances on the average ionic radii of the La-*R*123 mixed compounds (open squares) compared to the *R*123 ones (solid squares, Ref. 5).

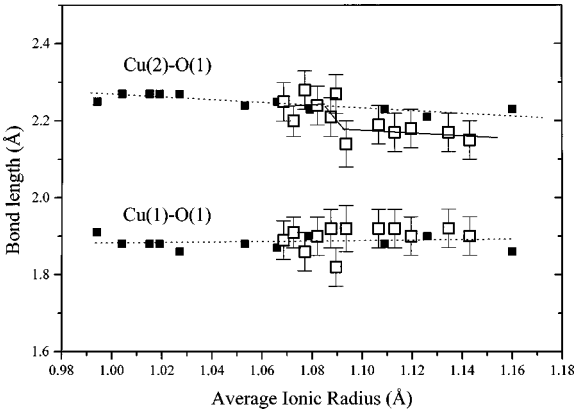

FIG. 3. Dependence of the Cu(2)-O(1) and Cu(1)-O(1) distances on the average ionic radii of the La-*R*123 mixed compounds (open squares) compared to the *R*123 ones (solid squares, Ref. 5).

*R*123 compounds up to an approximate average ionic radius 1.09 Å that corresponds to Y and then for larger rare-earth elements the Cu(2)-Cu(2′) slots are greater and the Cu(1)-Cu(2) distances are slightly smaller than expected from the *R*123 series. Thus, for the mixed compounds with r_R greater than 1.09 Å, the central La-*R* cage is under tensile strain while the Ba cage is under slight compressive strain, compared to the corresponding *R*123 compounds. The strain seems to relax for the second half of the rare-earth atoms with the bond lengths having values that correspond to the *R*123 phase if scaled to the average ionic radius. This could be related to the separation of phases as it is discussed below. For the Pr-*R*123 compounds[5] it is worth noticing that the corresponding values of the Cu(2)-Cu(2′) slots are lower than expected from the *R*123 data.

The modification of the Cu(2)-Cu(2′) distance is mostly attributed to corresponding changes of the Cu(2)-O(1) bond (i.e., the apical oxygen O(1) comes closer to the CuO_2 planes) because the Cu(1)-O(1) bond values fit to those expected for the single *R*123 compound (Fig. 3). The different effects that La and Pr have on the interatomic distances can already be seen (Fig. 1). Both Pr and La do not follow their ion size trend (Fig. 1) with Pr behaving as a much smaller ion and La as a larger one in the case of the *R*123 compounds. This forces the Cu(2)-Cu(2′) interatomic distances in the mixed compounds to be drawn towards smaller (Pr) or larger (La) values than their formal ion size.

Within the cuprate block the average *R*-O(2,3) bond distance for all mixed La-*R*123 compounds is smaller than the corresponding one for the single *R*123 compounds. Thus the presence of La seems to induce shortening of the *R*-O(2,3) bonds. Such an effect has not been observed in the mixed Pr-*R*123 compounds.[5]

The *R*123 compound has a strained tri-perovskite-like structure. One expects that the mixed La-*R*123 compounds under investigation are additionally strained in forcing the different blocks of the unit cell of the mixed crystal to be commensurate. In the La-*R*123 compounds different factors affect the additional strain. First, the difference in ionic size between the large La and the other *R* ion induces a strain between adjusted unit cells. For instance, if the La and *R* unit cells are forced to adjust on the *a* and *b* axes, they will be strained even in the *c*-axis direction, due to the vertical dis-

placement of the O(2,3) atoms. The *a* (or *b*) axis mismatch between La123 and *R*123 ranges from 0.75% (or 0.47%) for La-Nd to 2.14% (or 1.5%) for La-Tm. Overdoping with oxygen of the La-*R*123 mixed compounds, which is expected by the preparation conditions and is supported from the softening of the in-phase mode in the Raman spectra, should be another factor inducing strain. For pure $YBa_2Cu_3O_y$ with high oxygen content $y \approx 7$ it has been shown[16] that the structure should be close to instability with the Ba atom being in a cavity that is too small.

In La-*R*123 for the first half of the rare-earth atoms (*R* = Pr, Nd, Sm, Eu, Gd, Dy) the strains due to overdoping can be partially relieved by substitution of Ba for the smaller La and *R* ion.[6] This substitution should also be accompanied with oxygen rearrangements among the O(1), O(4), and O(5) crystal sites.[17] Further strain relaxation in those samples can occur by the formation of different phases related with the oxygen concentration. Moreover, the mismatch between La and *R* cubes in the unit cell is relatively low for those compounds. Therefore for the first half of the rare-earth atoms we expect that the total strain is below the critical value and the mixed-phase La-*R*123 has been formed, although strained, as can be seen in Figs. 1–3.

For the second half of the rare-earth atoms (*R* = Lu, Yb, Tm, Er, Ho) and for Y, the mismatch between La and *R* cubes in the unit cell increases considerably, increasing the strain of the mixed La-*R*123 structure. At the same time the partial relief of strains in the Ba cage by the rare-earth substitution is smaller since the latter ceases to exist at Y.[6] Therefore the strains (due to overdoping and difference in ionic size between La and *R*) in the mixed phase La-*R*123 should be overcritical for *R* = Y, Ho, Er, Tm, Yb, and Lu. Full relaxation of the additional strains for those compounds occurs by mechanisms such as the creation of crystal defects (dislocations) and/or the formation of chemically separated phases rich in either La, *R*, or an intermediate phase. The latter is evident from the B_{1g} Raman-active mode of the out-of-phase vibrations of the plane oxygen atoms discussed below. Interatomic distances obtained by XRD should then relax to those of the average *R*123 phase scaled for the average ionic radius.

By inspection of the interatomic distances obtained by the XRD analysis one can see that the bonds that can probe the strain relaxation in the mixed La-*R*123 compounds are those with the plane oxygen O(3). This oxygen atom is situated along the *a* axis where the vacant O(5) sites are. It seems that the Ba-O(3), *R*-O(3), and Cu(2)-O(3) bonds accommodate most of the strain in the mixed La-*R*123 phase while bonds with O(2) along the *b* axis are less affected by the internal stress. Figure 4 shows the Ba-O(3) and *R*-O(3) distances as a function of average ionic radius r_R compared with the single-phase *R*123 data from Ref. 5. It is clear that the Ba-O(3) distances are stretched and the *R*-O(3) distances are compressed as compared to the *R*123 phase for r_R greater than 1.09 Å while both become equal to the expected *R*123 values if scaled to the average ionic radii for values smaller than 1.09 Å.

In Fig. 5 we have also plotted the Cu(2)-O(3) values for the Pr-*R*123 mixed phase from Ref. 5 for comparison with the La-*R*123. It is evident that the Cu(2)-O(3) distance is also strained for r_R greater than roughly 1.09 Å, relaxing to

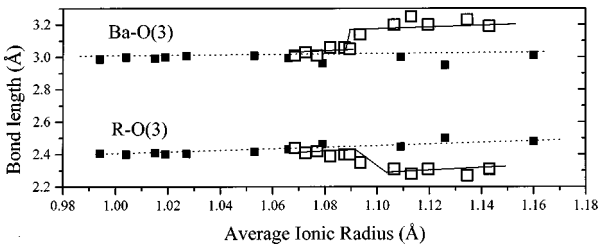

FIG. 4. Dependence of the Ba-O(3) and *R*-O(3) distances on the average ionic radii of the mixed La-*R*123 compounds (open squares) compared to the *R*123 ones (solid squares, Ref. 5).

the *R*123 values for smaller r_R. For those compounds, Raman studies have shown the existence of phases rich in the two rare-earth atoms. However, if we define the additional strain of bond distances as $s = (d_{\mathrm{str}} - d_{R123})/d_{R123}$, where d_{str} is the value of the strained bond distance in the mixed phase and d_{R123} is the corresponding value of the single *R*123 phase scaled over the average ionic radius, we see that *s* is positive for La-*R*123 and negative for Pr-*R*123. The additional strain is thus tensile for La-*R*123 and compressive for Pr-*R*123. This can be understood since the additional strain seems to depend on other factors, such as the oxygen concentration, the substitution for Ba, and the preparation conditions, besides the difference in ionic radii. The strain of the Cu(2)-O(3) bond affects also the puckering of the CuO_2 planes with the La-*R*123 strained mixed phases having anomalously low values and Pr-*R*123 high values of puckering angle.[5] On the other hand, comparing our sample of La-Pr123 with Pr-La123 of Ref. 5, we see that, despite the different strain in the Cu(2)-O(3) bond that proves the role of the preparation conditions, both samples show the same well-known ''anomaly'' of the *c* axis.

Therefore all these differences induced by the two ions of similar size, indicate that the structural changes of the La-*R*123 and Pr-*R*123 compounds are not due only to the size of the La or Pr ion. Other effects should be involved, such as the valence of the rare earth, the amount of oxygen content, etc. Moreover, since the phase separation depends on the total strain, the above results indicate that in these mixed compounds the mechanism for phase formation is not a pure ion-size effect.

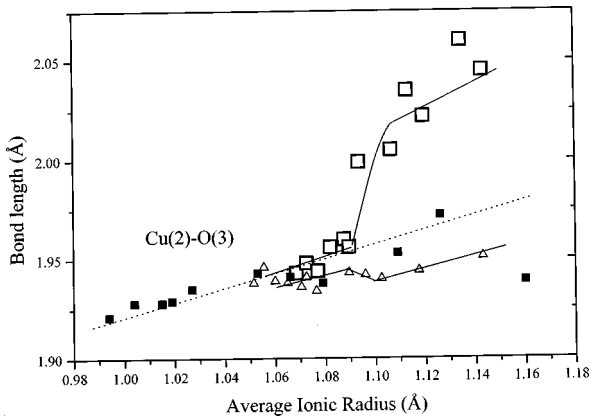

FIG. 5. Dependence of the Cu(2)-O(3) distances on the average ionic radii of the mixed La-*R*123 compounds (open squares) compared to the *R*123 (solid squares) and the Pr-*R*123 (open triangles) from Ref. 5.

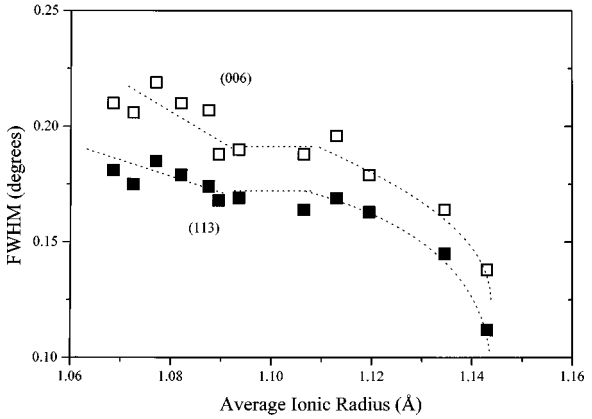

FIG. 6. Full width at half maximum (FWHM) of the (113) (solid squares) and (006) reflections (open squares) as a function of the average ionic radii of the mixed La-R123 compounds. Dotted line is a guide to the eye.

Figure 6 presents the width (full width at half maximum) of two diffraction lines obtained from the Rietveld refinement as a function of the average ionic radius. For all samples, the widths are larger than the corresponding ones of R123 and increase with decreasing average ionic radius. The broadening of the diffraction lines is expected if the crystallites are elastically distorted or the material is broken in smaller, coherently diffracting, domains. We propose that in our La-R123 samples and for the first half of the rare-earth atoms (R=Pr, Nd, Sm, Eu, Gd, Dy) the broadening is mainly caused by the elastically strained crystallites as discussed above. From Fig. 6 it is clear that the broadening reaches a limiting value at approximately 1.09 Å and for the second half the width does not retain the initial value but slightly increases further. This is an indication that the strain relaxation occurs for those compounds through mechanisms such as creation of crystal defects (dislocations) and/or decrease of the coherently diffracting domain size since both result in broadening of the diffraction profile. The creation of dislocations is probable because it always accompanies the relaxation of misfit strains, while the formation of phases rich in either La, R, or an intermediate phase would result in a decrease of the coherently diffracting domain size. Furthermore, the size of these domains should be small (<200 Å), otherwise the La123 and R123 phases would be detectable as a peak splitting in the diffraction lines at least for combinations such as La-Tm.

B. Raman measurements

Figures 7(a) and 7(b) present the micro-Raman spectra in the $y(zz)\bar{y}$ and $y(xx)\bar{y}$ scattering geometries, respectively. In the $y(xx)\bar{y}$ configuration, the phonon that is due to the Ba vibrations shows a considerable Fano-type asymmetry [Fig. 7(b)], while the peak that is due to the Cu vibrations (150 cm^{-1}) has very low intensity. These features, if compared with the pure Y123 compounds,[18] indicate that the samples have very good oxygenation ($y \geq 6.85$).

In the other scattering geometry [Fig. 7(a)], the Cu(2) phonon is constant in frequency, but the phonon of the Ba atom shows some structure in some compounds (i.e., La-Dy123) or it appears shifted to a higher frequency (~126 cm^{-1} for La-Pr123). Figure 8 shows three rare-earth combinations and the deoxygenated pure Y123 for comparison. It is clear that the ~126 cm^{-1} is a new line that appears either by some rare-earth substitutions or by the loss of oxygen.[18,19] The stability of the Cu(2) phonon frequency in the La-R123 compounds compared with the deoxygenated Y123 (Fig. 8) proves that in the rare-earth-substituted samples the appearance of the ~126-cm^{-1} line is not connected with any kind of oxygen loss. It is possibly connected with a mode that is activated by the substitution in these compounds or the loss of oxygen in pure Y123.[18,19] Since it does not appear in the fully oxygenated pure Y123 compound, it may be related with the partial substitution of Ba by a rare earth. One should

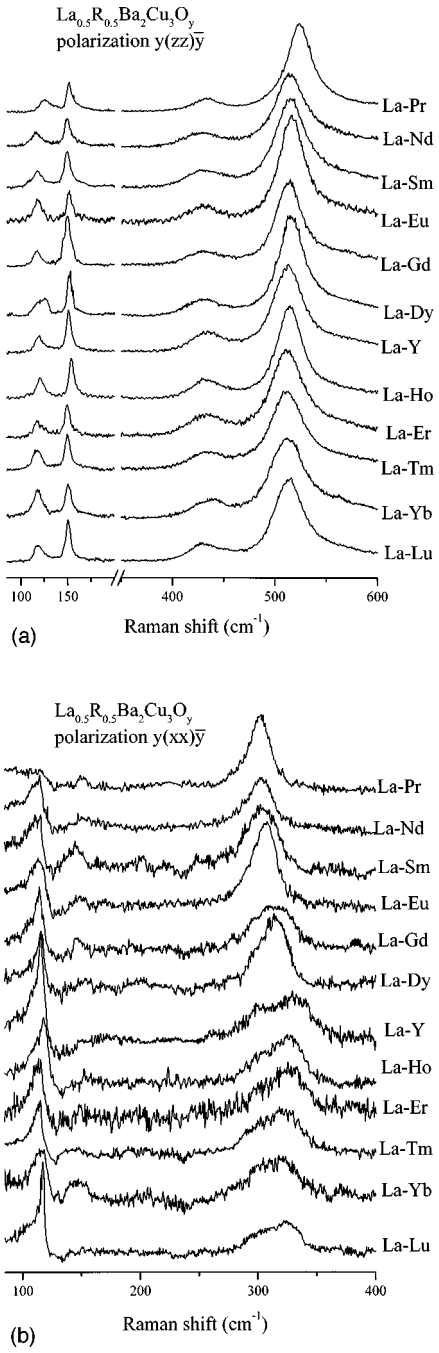

FIG. 7. Typical room-temperature micro-Raman spectra in the $y(zz)\bar{y}$ (a) and $y(xx)\bar{y}$ (b) scattering geometries for the $La_{0.5}R_{0.5}Ba_2Cu_3O_y$ samples.

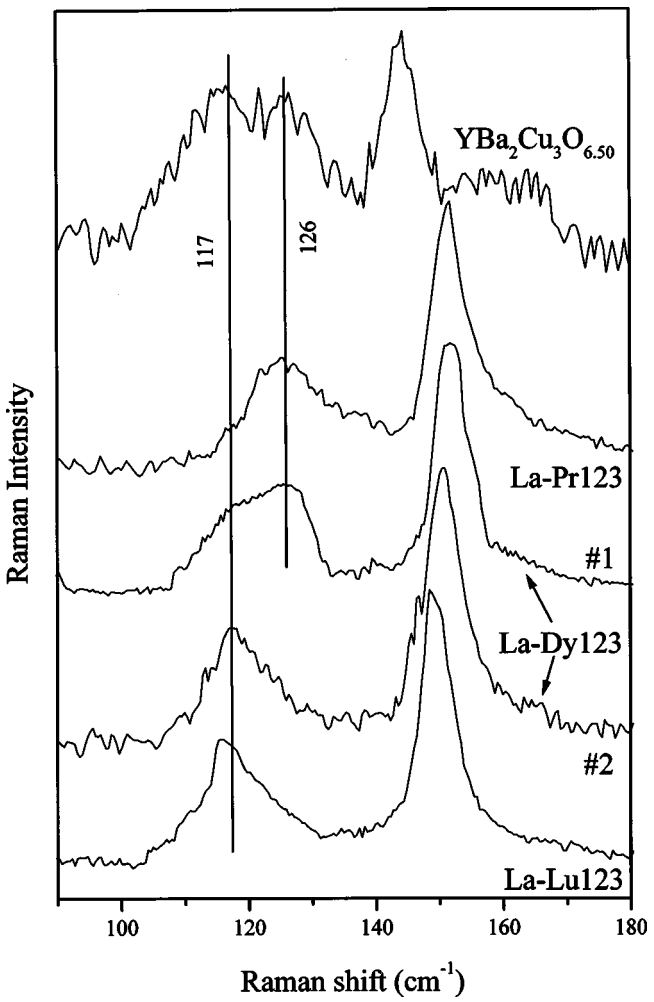

FIG. 8. The low-frequency region of the $y(zz)\bar{y}$ scattering configuration for the La-Lu123, La-Dy123 (two different microcrystallites), La-Pr123, and the deoxygenated pure $YBa_2Cu_3O_{6.5}$.

additionally note the variations detected among different microcrystallites for the same compound (Fig. 8) that point to the importance of the preparation conditions.

Figure 9 presents the variation of the phonon frequencies due to the apical oxygen and the O(2,3) in-phase vibrations with respect to the average ionic radii of La and *R* compared with the relative results of the pure *R*123 compounds.[20,21] As in the case of Pr-*R*123, the apex phonon appears as a wide peak at average frequencies that agree with the results of the *R*123 compounds. Its width increases with decreasing average ionic radius, being always larger than ~ 30 cm^{-1} (Fig. 10), which in pure Y123 samples corresponds to strongly disordered chains like those obtained by deoxygenation.[18] The increase of the apex phonon width with decreasing ionic radii of La and the *R* can be also attributed to the separation of phases rich in the two rare-earth atoms, but the dependence of the apex phonon frequency on the size of the rare-earth ion is not strong enough (Fig. 9) to allow the study of the phase-separation mechanism based on the apex phonon characteristics.

The frequency of the in-phase mode does not depend on the ionic radius (Fig. 9) as was the case in the Pr-*R*123 system.[4] On the other hand, in all compounds of the La-*R*123 series (including Pr-La123) the in-phase mode ap-

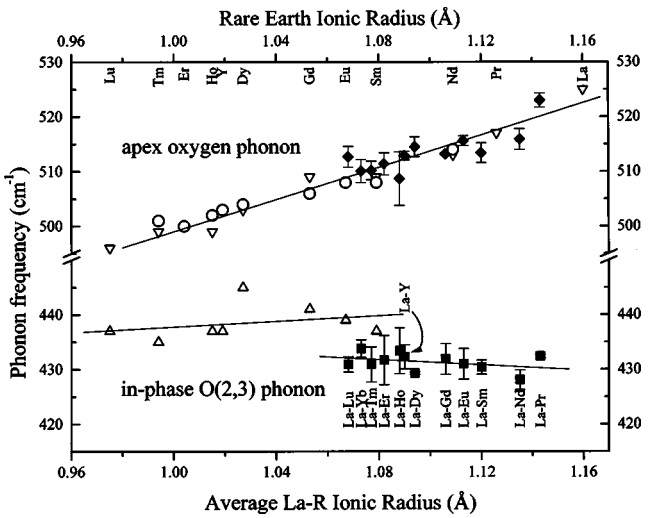

FIG. 9. Variation of the apex (solid diamonds) and the O(2,3) in-phase (solid squares) phonon frequencies for $La_{0.5}R_{0.5}Ba_2Cu_3O_y$, with respect to their average La-*R* ionic radii, together with the relative results for the pure $RBa_2Cu_3O_y$ compounds [open up and down triangles (Ref. 20) and open circles (Ref. 21)]. Best linear fits are also shown.

pears at a low value (431 ± 2 cm^{-1}) compared with previous *R*123 measurements[20,21] or the Pr-*R*123 system.[4] Up to now, a softening of the in-phase mode by 6–7 cm^{-1} was detected in oxygen-overdoped $YBa_2Cu_3O_y$ samples in going from $y = 6.92$ to $y = 6.98$ and proved to be due to a phase-transition mechanism originating from the excess oxygen.[22] In the present case, the association of the softening of the in-phase mode with an increase of the oxygen content beyond its optimum value ($y \cong 6.92$) will agree with the XRD data discussed above and the preparation conditions.[9] Based on the Raman measurements for the other combinations of the rare-earth atoms that do not show any softening for the in-phase mode[4] one can conclude that it is only La that has this tendency to attract more oxygen.[9]

Besides the softening, it can be seen in Fig. 10 that the width of the in-phase mode exceeds 40 cm^{-1} for all rare-

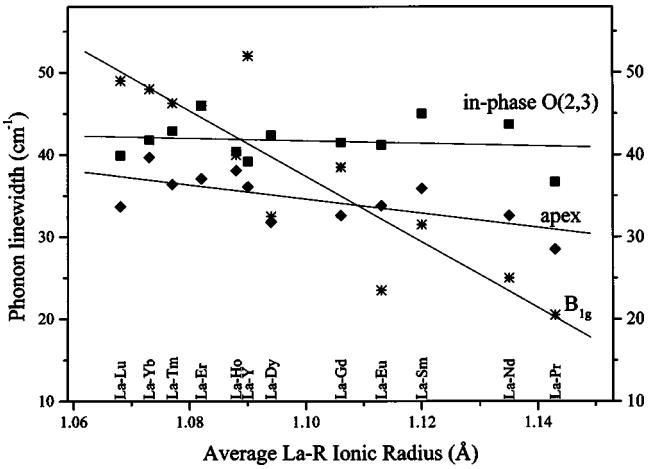

FIG. 10. Variation of the apex (solid diamonds) and the O(2,3) in-phase (solid squares) and out-of-phase (stars) phonon linewidths of $La_{0.5}R_{0.5}Ba_2Cu_3O_y$ (each fitted with one Lorentzian) with respect to the average ionic radius.

earth combinations, which is considerably larger than the maximum value (<30 cm^{-1}) observed in pure Y123.[18] In that case, the increase of the phonon width towards optimum doping was associated with the formation of new phases.[22] The softening of the in-phase mode in connection with its large width in the present systems could also indicate the appearance of many phases associated with different oxygen concentrations. This is consistent with the structure of the in-phase mode that is evident in some rare-earth combinations [Fig. 7(a)]. One could assume that any phase that includes La corresponds to high oxygen (overdoped) concentrations while the $R123$ phases are associated with the lower (optimally or underdoped) oxygen concentrations. The location of the average phonon frequency of the in-phase mode at values that correspond to oxygen overdoping is an indication of the existence, in considerable amounts, of phases rich in lanthanum (La123 or mixed La-$R123$).

The possible partial substitution of La and/or R for Ba could have the tendency to attract oxygen if the rare-earth atoms prefer a higher coordination than Ba. This higher coordination could be achieved by filling the O(5) site in the Cu(1) planes along the a axis, increasing the oxygen concentration and inducing the softening of the in-phase mode. Any filling of the O(5) site would tend to decrease the orthorhombicity of the compound, and therefore should be detected by the XRD data. On the other hand, the absence of any softening of the in-phase mode for other combinations of rare-earth atoms that substitute for Ba (Ref. 4) does not support any correlation of the partial rare-earth substitution for Ba with this softening. An alternative could be that La causes structural modifications such as increase of the puckering, decrease of the La-O(3) distances, etc., which are related to the in-phase phonon softening and are similar to those induced by the excess of oxygen.[22] Since the preparation conditions support the hypothesis of excess in the oxygen concentration,[9] it is reasonable to assume that the softening is mainly related to the excess of oxygen. The structural changes observed should be the result of combined phenomena, such as the increase of the oxygen content, the size of the rare earth ion, and the possible substitution of a rare-earth ion for the large Ba atom without excluding any dependence on the preparation conditions.

In the (xx) polarization spectra, a considerable broadening and a gradual shift in frequency of the B_{1g} phonon is observed [Fig. 7(b)] as the difference between the ionic radii of La and the other rare earth increases. When the average position of this mode is plotted against the average ionic radius (Fig. 11), it follows the trend of the pure $R123$. On the other hand, the considerable increase of the phonon width (Fig. 10) and the obvious structure in some rare-earth combinations (i.e., for La-Y123) is similar to the Pr-$R123$ compounds.[4] In that work the large broadening of the B_{1g} phonon was attributed to the existence of two or three phases corresponding to areas rich either in Pr, the other rare earth, or to a mixed state.[4,23] Such a mixture of phases was detected when the difference in the ionic radii[15] exceeded a limiting value favoring the separation of phases and explaining the appearance of superconductivity in those compounds.[4]

Similar phases could exist in the La-$R123$ compounds that can be studied from the B_{1g} phonon characteristics because its frequency is very sensitive to the rare-earth ion size

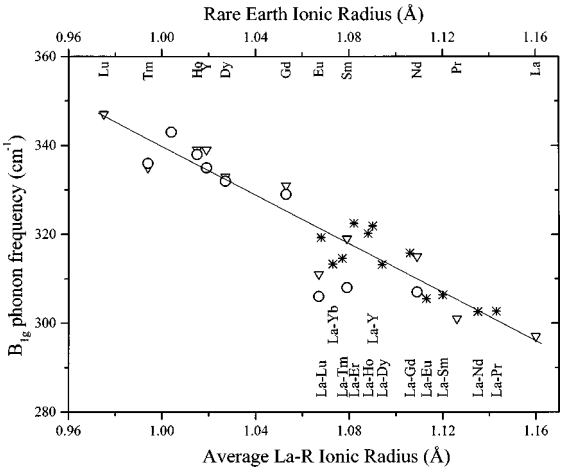

FIG. 11. Variation with the (average) ionic radius of the B_{1g} phonon frequency of $La_{0.5}R_{0.5}Ba_2Cu_3O_y$ (fitted with one Lorentzian, stars), and $RBa_2Cu_3O_y$ [open down triangles (Ref. 19), open circles (Ref. 20)]. The best linear fit for Ref. 19 is shown.

(Fig. 11). As can be seen in Fig. 7(b), starting from the La-Y123 compound a structure becomes obvious, which persists in the heavier rare-earth elements. This is in qualitative agreement with the characteristic changes that have been observed in the XRD data discussed above. The attempt to fit the B_{1g} band by two Fano-shaped modes that would correspond to the B_{1g} modes of La123 and $R123$ is not successful, and one is forced to assume the existence of a third peak at an intermediate frequency. We have therefore to assume the separation into at least three phases when the difference in the ionic radius of the two rare-earth atoms exceeds a limiting value. This hypothesis agrees with the assumption of internal strains that are developed by the misfit of the La123 and $R123$ unit cells and relax by a phase-separation mechanism.

This mechanism should be more complicated than originally assumed[4] because for some compounds (e.g., La-Lu123) there is not much of a trace of a Lu123 mode, which implies that there is no separation of the pure Lu123 phase. When this is compared with the case of the Pr-Lu123 mixed compound,[4] it is seen (Fig. 12) that there the pure Lu123 phase is separated leading to the superconductivity of the compound, while for La-Lu123 there is no isolation of the Lu123 phase, though the difference in the ionic radius of La-Lu is greater than that of Pr-Lu. It is therefore reasonable to assume that the phase-separation mechanism is much more involved than a pure geometrical factor that depends only on the difference of the two ionic radii. If it is related with the development of internal strains, it can be also associated with the amount of oxygen content, the possible substitution of Ba by the rare-earth atom, and the preparation conditions.

Therefore, the results indicate that there are many mechanisms of phase formation, arising not exclusively from the difference in the ionic radii of the two rare-earth atoms. It is quite probable that the built-up strains from various phenomena are the main reason for the system to break into microdomains of different stoichiometry as a critical difference of ionic radius for the two rare-earth atoms is reached, leading

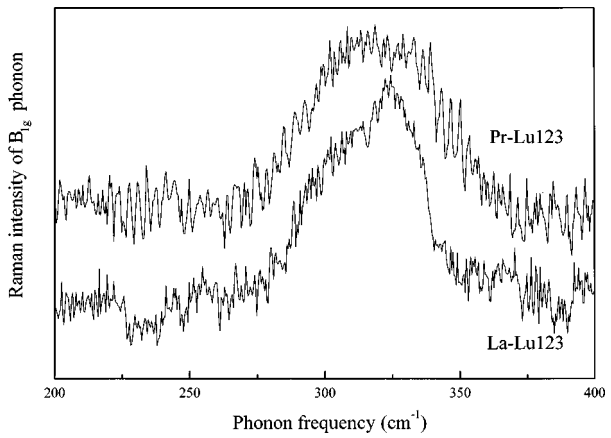

FIG. 12. Typical room-temperature micro-Raman spectra in the $y(xx)\bar{y}$ scattering geometry for the $La_{0.5}Lu_{0.5}Ba_2Cu_3O_y$ and the $Pr_{0.5}Lu_{0.5}Ba_2Cu_3O_y$ samples.

to the reappearance of superconductivity in the Pr-*R*123 systems. For the La-*R*123 compounds there is no disappearance of superconductivity, but there is a different behavior of the interatomic distances from that of the Pr-*R*123 systems due to the various underlying mechanisms that induce the internal strains.

IV. CONCLUSIONS

Remarkable changes are induced in the Raman spectra due to the substitution of La for another rare earth, i.e., the broadening and shift of the B_{1g} and the softening of the in-phase vibrational modes of the plane oxygen atoms. The first effect seems to be correlated with the development of phases rich either in La, or in *R*, or in an intermediate phase. The phase separation could be probed by the strain relaxation of the different interatomic distances obtained by XRD analysis. The separation of the phases seems to depend not only on the difference of the rare-earth ionic radii, but also on the specific combination of the elements. Concerning the softening of the in-phase mode, the data up to now indicate that it is related to an oxygen concentration beyond its optimum value. Changes observed in the CuO_2 planes in the Pr123 and Pr-*R*123 compounds are not due only to the size of the Pr ion. Other effects should be involved, such as the valence of the rare earth, the amount of oxygen content, etc.

ACKNOWLEDGMENTS

One of us (D.P.) would like to express his appreciation for financial support to the State Scholarships Foundation (''IKY'') of Greece. Thanks are due to Dr. A. Nabialek (Polish Academy of Sciences, Warsaw) for the magnetic characterization of the samples.

[1] H. B. Radousky, J. Mater. Res. **7**, 1917 (1992).
[2] H. A. Blackstead, D. B. Chrisey, J. D. Dow, J. S. Horwitz, A. E. Klunzinger, and D. B. Pulling, Phys. Lett. A **207**, 109 (1995).
[3] M. J. Kramer, K. W. Dennis, D. Falzgraf, R. W. McCallum, S. K. Malik, and W. B. Yelon, Phys. Rev. B **56**, 5512 (1997).
[4] G. Bogachev, M. Abrashev, M. Iliev, N. Poulakis, E. Liarokapis, C. Mitros, A. Koufoudakis, and V. Psyharis, Phys. Rev. B **49**, 12 151 (1994).
[5] G. D. Chryssikos, E. I. Kamitsos, J. A. Kapoutsis, A. P. Patsis, V. Psycharis, A. Koufoudakis, Ch. Mitros, G. Kallias, E. Gamari-Seale, and D. Niarchos, Physica C **254**, 44 (1995).
[6] W. Wong-ng, B. Paretzkin, and E. R. Fuller, J. Solid State Chem. **85**, 117 (1990).
[7] T. B. Lindemer, B. C. Chakoumakos, E. D. Specht, R. K. Williams, and Y. J. Chen, Physica C **231**, 80 (1994).
[8] T. Wada, N. Suzuki, T. Maeda, S. Uchida, K. Uchinokura, and S. Tanaka, Appl. Phys. Lett. **52**, 1989 (1989).
[9] T. Wada, N. Suzuki, S. Uchida, and S. Tanaka, Phys. Rev. B **39**, 9126 (1989).
[10] M. H. Ghandehari and S. G. Brass, J. Mater. Res. **4**, 1111 (1989).
[11] S. A. Howard, Computer code RIET, Department of Ceramic Engineering, University of Missouri-Rolla, MO, 1988.
[12] J. D. Jorgensen, B. W. Veal, A. P. Paulikas, L. J. Nowicki, G. W. Crabtree, H. Claus, and W. K. Kwok, Phys. Rev. B **41**, 1863 (1990).
[13] *The Rietveld Method*, edited by R. A. Young (Oxford University, New York, 1993).
[14] N. Guskos, V. Likodimos, C. A. Londos, V. Psyharis, C. Mitros, A. Koufoudakis, H. Gamari-Seale, W. Windsh, and H. Metz, J. Solid State Chem. **119**, 50 (1995).
[15] R. D. Shannon, Acta Crystallogr., Sect. B: Struct. Crystallogr. Cryst. Chem. **B25**, 925 (1976).
[16] I. D. Brown, J. Solid State Chem. **82**, 122 (1989).
[17] V. A. Atsarkin, G. A. Vasneva, and V. V. Demidov, Zh. Eksp. Teor. Fiz. **108**, 927 (1995) [JETP **81**, 509 (1995)].
[18] D. Palles, N. Poulakis, E. Liarokapis, K. Conder, E. Kaldis, and K. A. Müller, Phys. Rev. B **54**, 6721 (1996).
[19] G. Burns, F. H. Dacol, C. Feild, and F. Holtzberg, Solid State Commun. **77**, 367 (1991).
[20] H. J. Rosen, R. M. MacFarlane, E. M. Engler, V. Y. Lee, and R. D. Jacowitz, Phys. Rev. B **38**, 2460 (1988).
[21] M. Cardona, R. Liu, M. Bauer, L. Genzel, W. Konig, A. Wittlin, U. Amador, M. Baharona, F. Fernandez, C. Otero, and R. Saez, Solid State Commun. **65**, 71 (1988).
[22] E. Kaldis, J. Röhler, E. Liarokapis, N. Poulakis, K. Conder, and P. W. Loeffen, Phys. Rev. Lett. **24**, 4894 (1997).
[23] W. J. Zhu, P. Liu, and Z. X. Zhao, Physica C **199**, 285 (1992).